

A Supplementary Material

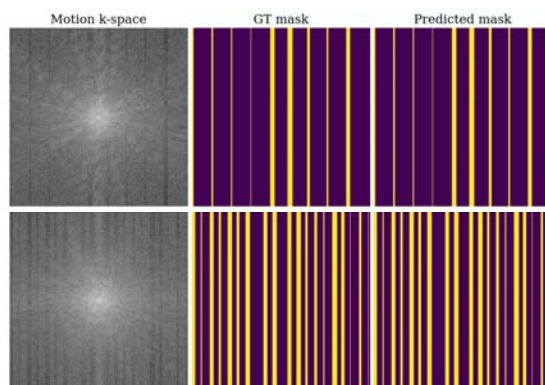


Fig. 3. k LD-Net detection results. The first and second show the detection performance of the k LD-Net for light and heavy motion, respectively.

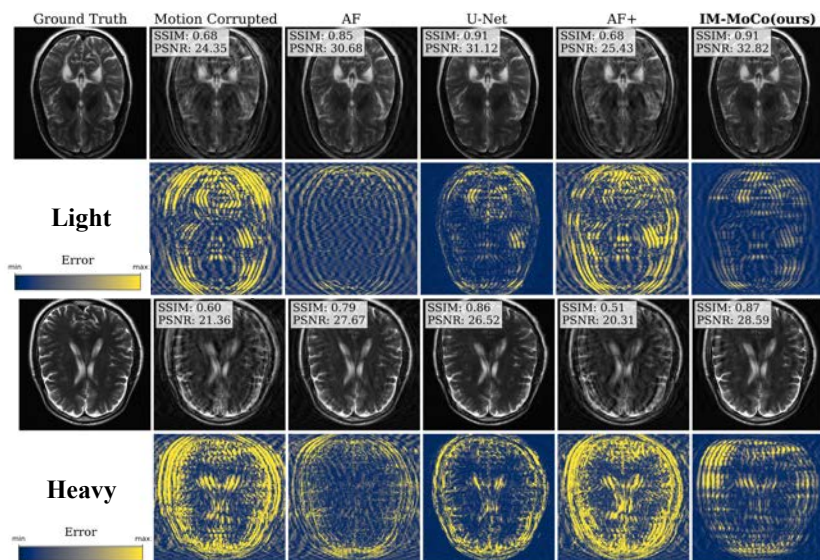


Fig. 4. The visualization shows the worst results of motion-corrected images of our IM-MoCo pipeline besides motion-corrupted, ground truth, and comparison methods. The first and third rows show the light and heavy correction results, respectively. The second and fourth rows show the residual error images.

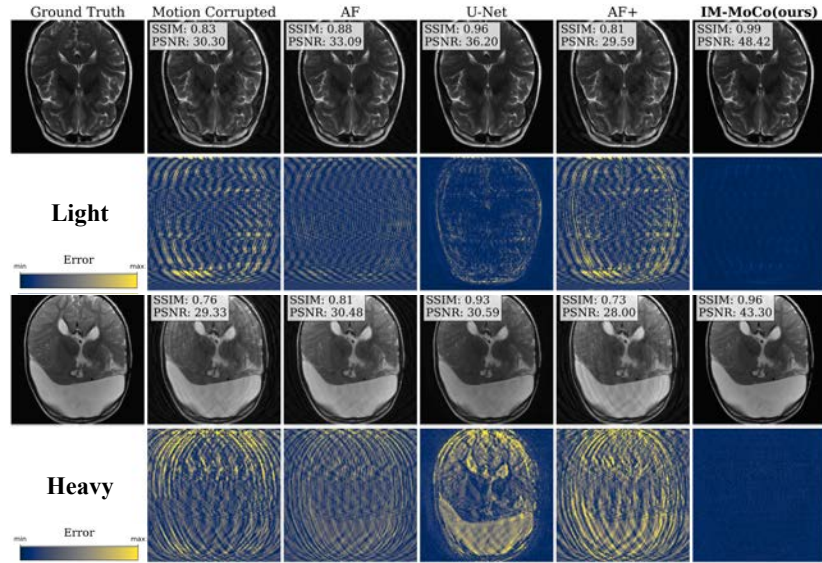


Fig. 5. The visualization shows the best results of motion-corrected images of our IM-MoCo pipeline besides motion-corrupted, ground truth, and comparison methods. The first and third rows show the light and heavy correction results, respectively. The second and fourth rows show the residual error images.

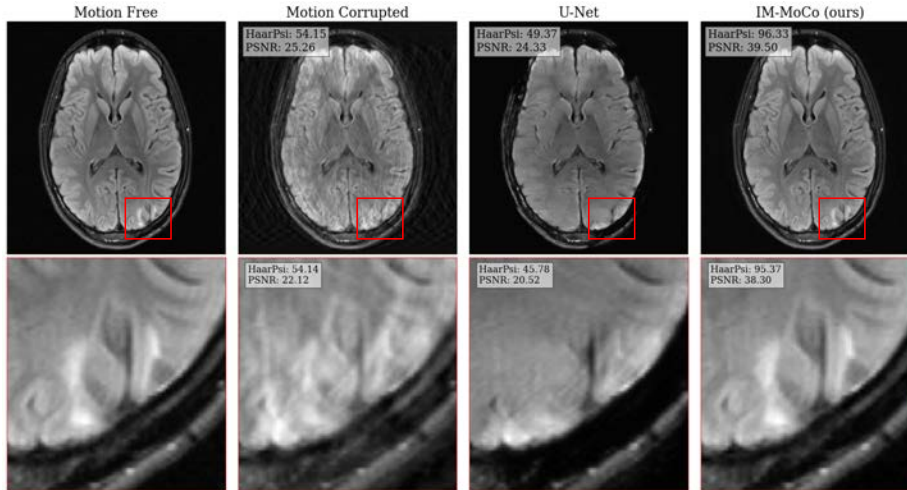


Fig. 6. A visualization of a *Non-specific white matter lesion* as an example. The first and second rows show the full image and the extracted patches, respectively.